



ARCHIVES  
of  
FOUNDRY ENGINEERING

ISSN (2299-2944)  
Volume 19  
Issue 3/2019

78 – 83

10.24425/afe.2019.127143

13/3



Published quarterly as the organ of the Foundry Commission of the Polish Academy of Sciences

# Primary Microstructure Characterization of As-Casted Co-20Ni-7Al-7W Superalloy

A. Tomaszewska, G. Moskal \*, T. Mikuszewski, G. Junak, A. Plachta

Silesian University of Technology, Institute of Material Science  
ul. Krasińskiego 8, 40-019 Katowice, Poland

\* Corresponding author. E-mail address: grzegorz.moskal@polsl.pl

Received 12.04.2019; accepted in revised form 18.07.2019

## Abstract

The primary microstructure of new Co-based superalloy of Co-20Ni-7Al-7W (at.%) type was showed in this article. The alloy was manufactured by induction melting in vacuum furnaces. This alloy is a part of new group of high-temperature materials based on Co solid solution and strengthened by coherent  $L1_2$  phase similar to Ni-based superalloys with  $\gamma'$  phase. The final form of  $Co_{ss}/L1_2$  microstructure is obtained after fully heat treatment included homogenization, solutionizing and aging processes. But first step of heat treatment thermal parameters determination is characterization of primary microstructure of alloys after casting process with special attentions on segregations of alloying elements in solid solution and presences of structural elements such as eutectic areas, and other phases precipitations. In analysed case the relatively high homogeneity of chemical composition was expected especially in the case of W distribution, what was confirmed by SEM/EDS analysis in dendritic and interdendritic areas.

**Keywords:** New Co-based superalloys, Co-20Ni-7Al-7W alloy, Primary microstructure

## 1. Introduction

Superalloys based on Ni or Co are high-performance materials used usually in high-temperature elements of gas turbines in aircraft engines or stationary units. These alloys are used in combustion chambers, discs, blades, vanes, rotating shafts and nozzle guide [1]. The advantages of the Co-based superalloys is related with their very good hot corrosion, wear, and oxidation resistance are required. In consequence they are used as critical turbine engine parts where those properties are critical requirements [2-4]. Their basics disadvantages are related with lower high temperature strength. This phenomena follows from lower effectivity of solid solution and carbide precipitation strengthening mechanism. This fact make them unusable for strongly loaded elements such as blade or disk. The preferential applications of Co-based superalloys are static parts such as vanes [2]. Recent investigations showed that there is possibility of  $\gamma/\gamma'$

structure creation in Co-based superalloys. In the Co-X (X=W, Nb, Ta) systems, a compounds  $Co_3X$  with  $L1_2$  type of structure ( $\gamma'$ ) in ordered form has been described [5-8], but the most important problem of this structural element is its thermal instability at temperature higher than  $> 600^\circ C$  [9-11]. The  $Co_3X$  order compound has a cuboidal morphology, and its precipitations are localized in the solid solution cobalt matrix similar to  $Ni_3(Al,Ti)$  ordered and stable compounds in the nickel based matrix [12], and transforms at higher temperature to equilibrium disordered form with the same formula  $Co_3X$  but with topological close packed morphology ( $D0_{19}$ ) [13-15]. Metastability of  $Co_3X$  phases with refractory elements can be weakened by formation of triple phases such as  $Co_3(Al,X)$ , what was firstly confirmed in the case of Co-Al-W alloys. Addition of alloying elements such as tungsten and aluminum to cobalt solid solution stabilizes the ordered  $L1_2$  lattice structure to temperature up to  $900^\circ C$  [9,10]. Basing on those considerations the new group of materials based on Co-Al-X systems where X are refractory elements such as W

(tungsten consists Co-Al-W alloys) were developed [9,10]. The main strengthening element in those alloys is ordered  $L1_2$  phase with overall formula  $Co_3(Al,X)$ . New Co-based superalloys strengthened by  $Co_3(Al,X)$  structural element with high thermal stability are characterized by solidus and liquidus temperatures higher than Ni-based superalloys, additionally they exhibit less tendency to alloying elements segregation during solidification process [16]. Addition of Ni to Co-based superalloys increased the limit of refractory elements as an alloying elements and the same decreased the susceptibility to formation TPC phases due to increasing of  $\gamma'$  field in ternary systems (thermal stability) Co-Al-X as well as the  $\gamma'$  solvus temperature. Additionally Ni addition improved the mechanical, creep and oxidation properties [17-21]. The Ni addition can be as high as 30 at.%.

## 2. Materials and experiment procedure

The nominal composition of analysed Co-20Ni-7Al-7W cobalt-based superalloy used in presented investigation is showed in Table 1. The induction vacuum process was used to alloy preparation. The process was made in furnace of VSG 02 Balzers type, and the alloy was manufactured in  $Al_2O_3$  crucible. The manually compacted moulding sand Konmix MAPI was used to set in of the alumina crucible in the furnace coil. Argon of ALPHAGAZ™ 1Ar (99,999% Ar) type was used to protection of liquid metal. Before the process start a operating chamber was washed by argon blowing (3 times), after this the working pressure was decreased to value of  $10^{-3}$  Tr ( $\sim 0,13$  Pa) and in the next step, the furnace chamber pressure was increased to operating 600 Tr ( $\sim 800$  hPa) by Ar filling. As a stock material, a technically pure metals were utilized: electrolytic Co and Ni (both min. 99,98%), Al 3N8 (99,98%) and W. The last element was, added with 20% surplus to require (from chemical composition) weight. Alloying elements such as Co, Ni and Al were added to crucible in first step, before the melting process. The last one element – W was being added to liquid solution of Co-Ni-Al after its high temperature homogenization. The final alloy was thermally treated in temperature range  $1650 \div 1750^\circ C$  by 10 minutes. Co-20Ni-7Al-7W final alloy was casted to the rods form under protective argon atmosphere into cold graphite moulds.

Table 1.

Nominal chemical composition of Co-20Ni-7Al-7W alloy

| Element | Co   | Ni   | Al  | W    |
|---------|------|------|-----|------|
| at. %   | 66,0 | 20,0 | 7,0 | 7,0  |
| wt. %   | 59,5 | 17,9 | 2,9 | 19,7 |

The phase constituent of obtained material was analyzed by X-ray diffraction method using X'Pert 3 diffractometer. Imaging of microstructure and chemical composition state were carried out by scanning electron microscopy equipped with an EDS apparatus on a Hitachi S-4200N microscopy. The light microscopic analysis of microstructure were made on Nikon Eclipse MA200 microscopy.

## 3. Results

The final products were two rods with size  $\varnothing 20 \times 100$  mm, showed in Figure 1. The rods were used to specimens preparation, and sectioned longitudinally and transversely to cast axis. Primary, analysis of chemical composition as well as the phase constituent of Co-20Ni-7Al-7W were made. The phase composition analysis of Co-20Ni-7Al-7W alloy in as cast state showed solely the presences of phase corresponding to Co solid solution with addition of Ni, W and Al (Figure 2). This hypothesis was confirmed by lattice parameter  $d$  value shifted to 2,0742 from 2,0467 typical for Co (ICDD pattern 15-0806), the proper value should equal 2,0467. Detailed evaluation of XRD pattern did not reveal the occurrence of XRD reflexes identified with nickel, aluminium and tungsten, which are alloying elements of investigated superalloy as well as any other phase which are the combinations of those elements. On the other hand, presence of those elements was confirmed by analysis of chemical composition using EDS method. The results of chemical composition analysis are present in Table 2. The concentration of aluminium and tungsten is little lower than was assumed, but it should be noted that this is data from EDS analysis.



Fig. 1 General view of final-cast from Co-Al-W alloy

Table 2.

Real chemical composition of Co-20Ni-7Al-7W alloy

| Element | Co   | Ni   | Al  | W    |
|---------|------|------|-----|------|
| at. %   | 67,6 | 21,3 | 5,7 | 5,4  |
| wt. %   | 62,3 | 19,6 | 2,4 | 15,7 |

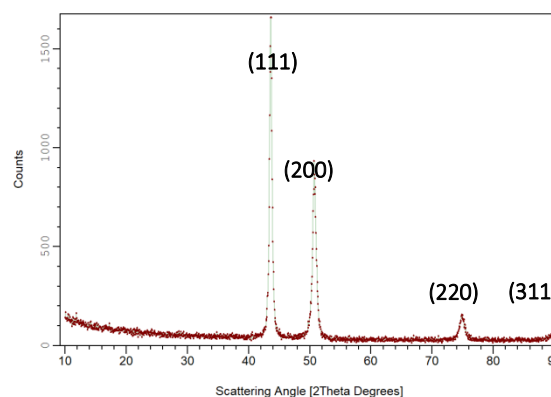


Fig. 2. Diffraction pattern of Co-2-Ni-7Al-7W alloy in as-cast state

Similar to the Co-9Al-9W alloy casting process [22] in this case the 20% tungsten excess relative to basic chemical composition was also used. Taking into consideration additionally the tendency to aluminium vaporization, we can clearly rate correctness of carried process.

Next part of primary microstructure investigation of casted Co-20Ni-7Al-7W alloy were related with observation of metallographic samples cut in accordance to Figure 1. The aim of this part was evaluation of microstructure homogeneity, as well as alloying elements distribution, in particular tungsten, which is typical technological problem concerning tungsten-rich alloys. The electrolytic etching in solution containing 25 ml H<sub>2</sub>O, 50 ml HCl, 15 g FeCl<sub>3</sub> and 3 g CuCl<sub>2</sub> × NH<sub>4</sub>Cl × 2H<sub>2</sub>O was used to microstructure disclosure. Primary structure of investigated superalloy at macroscale is shown in Figure 3.

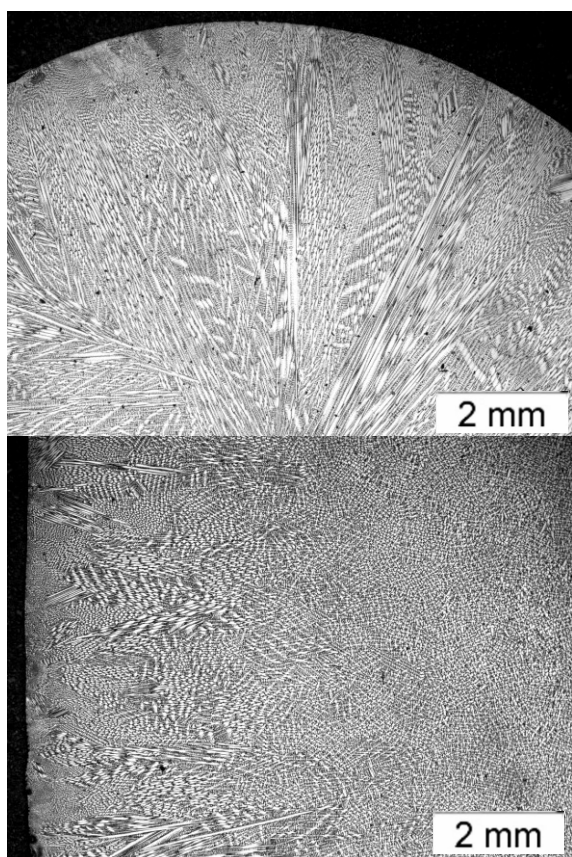


Fig. 3 View of dendritic microstructure of Co-20Ni-7Al-7W alloy on the transverse (up) and longitudinal (down) section

The primary structure visible in transverse section, consists of very thin, peripheral chill zone and wide columnar grains zone stretching to core of the casted rod. In this area, an equiaxed grains area were not found. In both longitudinal and transverse section, a direction of columnar crystals growth is according to direction of heat dissipation from solidifying ingot. Longitudinal section contains an area away from the bottom, where is present thick zone of fine, equiaxed grains, crystallized ahead of columnar front. This zone is much thicker than for Ni-free alloy

[22]. Revealed primary structure is typical for processes of fast and directionally solidifications with heat dissipation typical for casting into cold graphite moulds. Morphology of grains present in both mentioned crystal zones is shown in Figure 4.

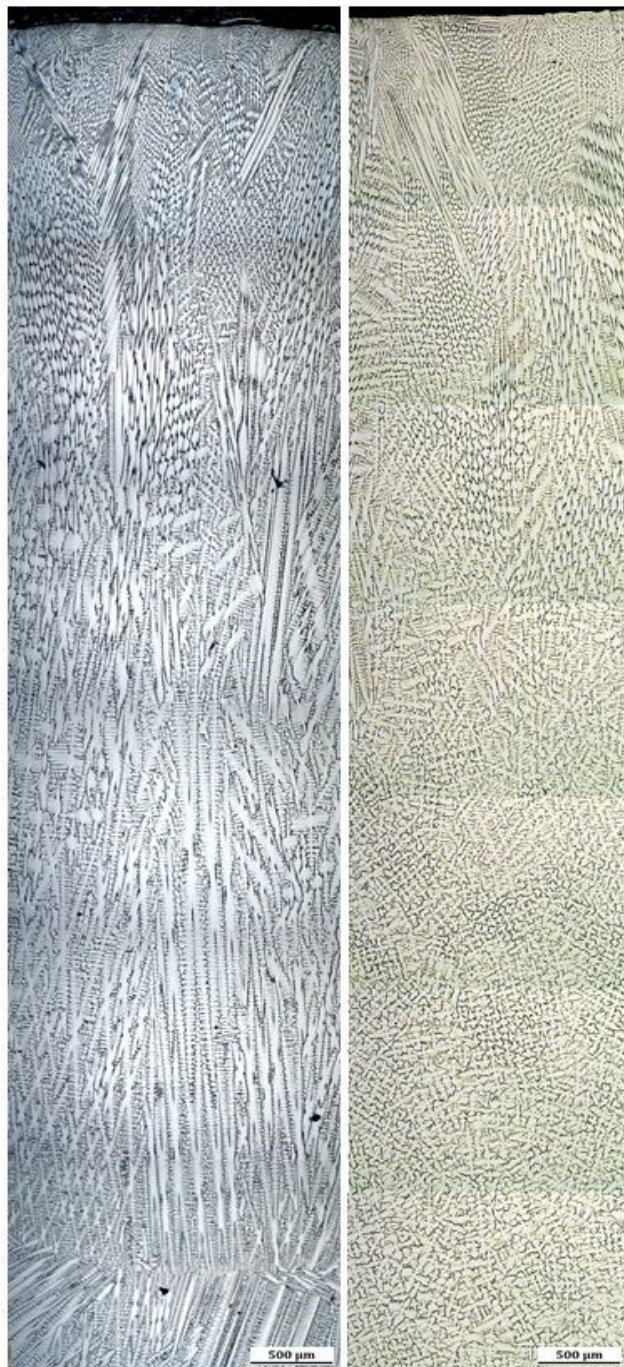


Fig. 4 Overall view of dendritic microstructure of Co-20Ni-7Al-7W alloy on the transverse (left) and longitudinal (right) section

The columnar zone is made of highly elongated dendritic cells with visible dendrites of first and second level type, and ovules of third level dendrites. Equiaxed grains zone consist of fine crystals of poorly expanded dendrites oriented randomly to other dendrites and to direction of heat dissipation (Figure 5).

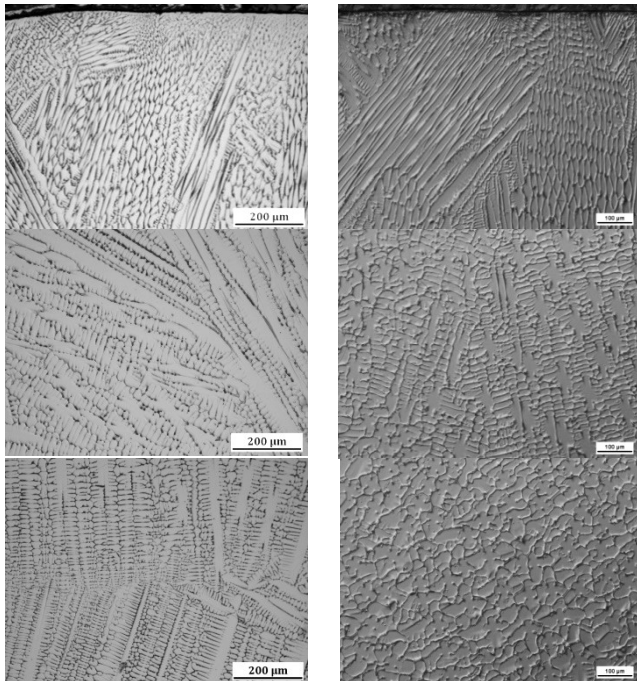


Fig. 5. Detailed view of dendritic microstructure of Co-20Ni-7Al-7W alloy on the transverse (left) and longitudinal (right) section in edge zone (up), middle zone (middle) and core (down)

Detailed results of chemical composition analysis obtained by EDS method and surface distribution of alloying elements such as tungsten, aluminium, nickel and cobalt for previously mentioned zones are presented respectively in Table 3 and Figure 6. Obtained results confirmed, that usage of technology including tungsten dosing into liquid cobalt-nickel-aluminium bath gives opportunity to obtain primary structure of Co-20-Ni-7Al-7W characterized by high homogeneity.

Table 3a.

Real chemical composition of dendritic areas in Co-20Ni-7Al-7W alloy

| Element   | Co   | Ni   | Al  | W    |
|-----------|------|------|-----|------|
| av. % wt. | 62,2 | 18,5 | 2,0 | 17,3 |
| max.      | 62,7 | 19,1 | 2,1 | 17,8 |
| min.      | 61,7 | 18,2 | 1,9 | 17,0 |
| av. % at. | 68,6 | 20,4 | 4,8 | 6,1  |
| max.      | 69,0 | 21,1 | 5,1 | 6,3  |
| min.      | 68,2 | 20,2 | 4,6 | 6,0  |

Table 3b.

Real chemical composition of interdendritic areas in Co-20Ni-7Al-7W alloy

| Element   | Co   | Ni   | Al  | W    |
|-----------|------|------|-----|------|
| av. % wt. | 62,5 | 20,8 | 2,8 | 14,0 |
| max.      | 63,0 | 22,2 | 3,2 | 15,3 |
| min.      | 62,0 | 19,6 | 2,3 | 11,8 |
| av. % at. | 66,6 | 22,2 | 6,4 | 4,8  |
| max.      | 68,0 | 23,3 | 7,2 | 5,3  |
| min.      | 65,6 | 21,3 | 5,4 | 3,9  |

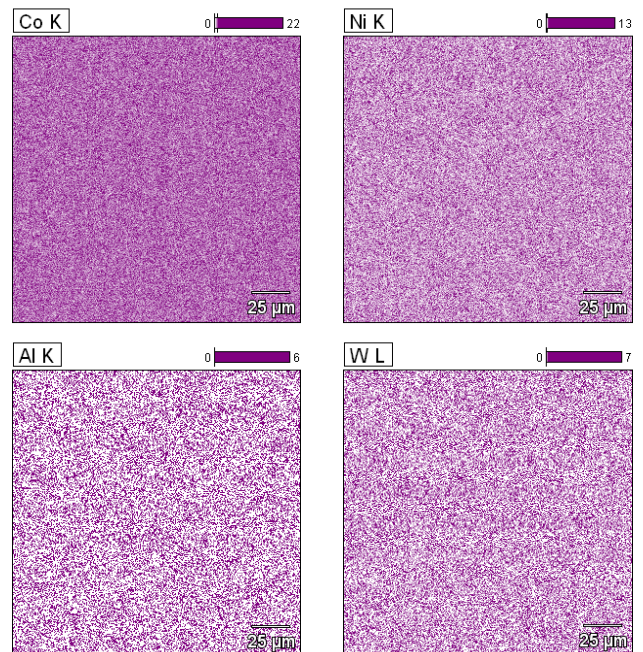
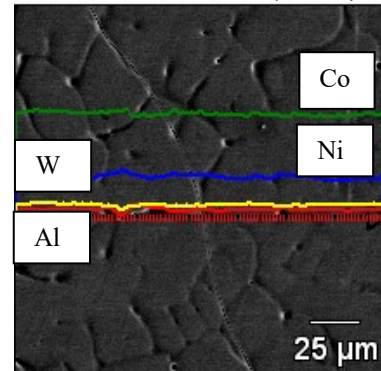


Fig. 6. Alloying elements linear and surface distribution in Co-20Ni-7Al-7W alloy

In particular, it concerned tungsten, whose distribution in primary structure is important technological issue and causes necessity of additional homogenization treatment.

Obtained information's showed, that the diversity of tungsten concentration in dendrite cores and interdendritic areas did not exceed 3,3% wt. (1,3% at.). Cobalt behaved in analogue way to

tungsten, resulting in increased concentration in dendrites about 0,3 % wt. (2,0 % at.). Opposite variation were observed in case of aluminum and nickel concentration, where value of difference between interdendritic and dendritic areas achieved even 0,8 % wt. (1,6 % at.) and 1,8 % wt. (2,3 % at.) respectively.

The analysis of chemical elements distributions in alloys revealed that the primary structure of obtained Co-20Ni-7Al-7W cast is characterized by high homogeneity of alloying elements distribution both in the case of dendritic as well as interdendritic areas. This homogeneity is important from potential heat treatment requirements. In the case of low segregations effect the homogenization process can be omitted and only solutionizing with aging should be expected.

The final analysis was related with characterization of HV1 hardness distribution between equiaxed crystals zone and external surface (Figure 7). Examination showed stable level of hardness value – ca. 240 - 245 HV1. Obtained hardness results exhibit proper correlation with data concerning primary structure. Zone of relatively smaller equiaxed crystals was too small to make the measurement, contrary situation was observed in the case of equiaxed crystals zone. This situation is other than for described earlier Co-9Al-9W alloy where the primary microstructure dominated by unfavorable columnar zone is presences much stronger on the cross sectioned sample [22]. The situation where the columnar zone is thinner is more favorable, particularly regarding wrought alloys.

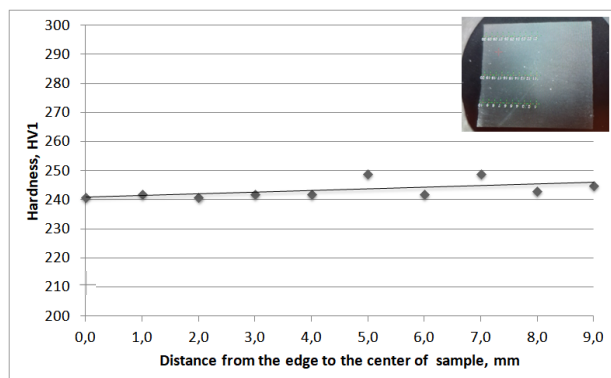


Figure 7 Hardness distribution on longitudinal cross section of Co-20Ni-7Al-7W superalloy

### 3. Conclusions

- Performed investigation showed, that Co-20Ni-7Al-7W alloy is characterized by relatively uniform primary structure compared to literature data especially from tungsten segregation point of view. This effect was achieved by tungsten dosing to molten metal bath of cobalt and aluminium during melting process. The differences in tungsten concentration in dendritic and interdendritic is ca. 2 at. %.
- The dominating microstructural element in the longitude cross sectioned specimen was equiaxed crystals, what is

beneficial effect from potential processes of wrought. This structural effect was confirmed by microhardness measurement where no significant differences were observed between columnar and equiaxed crystals.

- The analysis of microsegregation revealed slightly differences in aluminium and nickel content, wherein higher concentration of this element was observed in interdendritic zones.

### Acknowledgements

This work was supported partially by Faculty of Materials Engineering and Metallurgy, Institute of Materials Science of Silesian University of Technology, as a part of Statutory Research BK 221/RM0/2018 (11/990/BK\_18/0057) and partially by NCN (National Science Center Poland) as a part of “MINIATURA” project no 2018/02/X/ST8/01817.

### References

- [1] Reed, R.C. (2006) *The Superalloys Fundamentals and Applications*. Cambridge University Press.
- [2] Coutouradis, D., Davin, A. & Lamberigts M. (1987). Cobalt-based superalloys for applications in gas turbines. *Materials Science and Engineering A*. 88, 11-19. DOI:10.1016/0025-5416(87)90061-9.
- [3] Douglass, D.L., Bhide, V.S. & Vineberg, E. (1981). The corrosion of some superalloys in contact with coal chars in coal gasifier atmospheres. *Oxidation of Metals*. 16(1-2), 29-79. DOI: /10.1007/BF00603744.
- [4] Eliaz, N., Shemesh, G. & Latanision, R.M. (2002). Hot corrosion in gas turbine components. *Engineering Failure Analysis* 9(1), 31-43. DOI 10.1016/S1350-6307(00)00035-2.
- [5] Okamoto, H. (2008). Co-W (Cobalt-Tungsten). *Journal of Phase Equilibria and Diffusion*. 29(1), 119. DOI:10.1007/s11669-007-9229-0.
- [6] Okamoto, H., (2007). Co-Mo (Cobalt-Molybdenum), *Journal of Phase Equilibria and Diffusion*. 28(3), 300. DOI: 10.1007/s11669-007-9055-4.
- [7] Gupta, K.P. (2003). The Co-Nb-W (Cobalt-Niobium-Tungsten) system. *Journal of Phase Equilibria*. 24(1), 82-85. DOI: 10.1007/s11669-003-0018-0.
- [8] Gupta, K.P. (2003). The Co-Mo-Ta (Cobalt-Molybdenum-Tantalum) system. *Journal of Phase Equilibria*. 24(2), 186-189.
- [9] Sato, J., Omori, T., Oikawa, K., Ohnuma, I., Kainuma, R. & Ishida, K. (2006). Cobalt-base high-temperature alloys. *Science*. 312, 90-91. DOI:10.1126/science.1121738.
- [10] Lee, C.S. (1971). *Precipitation-hardening characteristics of ternary cobalt–aluminum–X alloys*. University of Arizona.
- [11] Korshynsky, M. & Fountain R.W. (1959). Precipitation phenomena in cobalt–tantalum alloys. *Transactions of the Metallurgical Society of AIME*. 215, 1033-1043.
- [12] Makineni, S.K., Nithin, B. & Chattopadhyay, K. (2015). A new tungsten-free  $\gamma$ - $\gamma'$  Co-Al-Mo-Nb-based superalloy.

- Scripta Materialia*. 98, 36-39. DOI:10.1016/j.scriptamat.2014.11.009.
- [13] Kokorin, V.V. & Chuistov, K.V. (1966). Initial stages of decomposition of supersaturated solid solutions Co-Ta and Co-Nb. *Fiz Metallov Metalloved.* 21, 311-314.
- [14] Dragsdorf, R.D. & Foreing, W.D. (1962). The intermetallic phases in the cobalt-tantalum system. *Acta Crystallographica*. 15, 531-536. DOI:10.1107/S0365110X62001371.
- [15] Dutkiewicz, J. & Kostorz, G. (1991). Structure of martensite in Co-W alloys. *Materials Science Engineering A*. 132, 267-272. DOI: 10.1016/0921-5093(91)90383-X.
- [16] Pollock, T.M., Dibbern, J., Tsunekane, M., Zhu, J. & Suzuki A. (2010). New Co-based gamma-gamma prime high-temperature alloys. *JOM*. 62(1) 58-63. DOI:10.1007/s11837-010-0013-y.
- [17] Liu, Q., Coakley, J., Seidman, D.N. & Dunand, D.C. (2016). Precipitate evolution and creep behavior of a W-free Co-based superalloy. *Metallurgical and Materials Transactions A*. 47, 6090-6096. DOI:10.1007/s11661-016-3775-1.
- [18] Shinagawa, K., Omori, T., Sato, J., Oikawa, K., Ohnuma, I., Kainuma, R. & Ishida, K. (2008). Phase equilibria and microstructure on  $\gamma'$  phase in Co-Ni-Al-W system. *Materials Transactions*. 49 (6), 1474-1479. DOI: 10.2320/matertrans.MER2008073.
- [19] Yan, H.-Y., Coakley, J., Vorontsov, V.A., Jones, N.G., Stone, H.J. & Dye, D. (2014). Alloying and the micromechanics of Co-Al-W-X quaternary alloys. *Materials Science and Engineering A*. 613, 201-208. DOI: 10.1016/j.msea.2014.05.044.
- [20] Neumeier, S., Freund, L.P. & Göken, M. (2015). Novel wrought  $\gamma/\gamma'$  cobalt base superalloys with high strength and improved oxidation resistance. *Scripta Materialia*. 109, 104-107. DOI: 10.1016/j.scriptamat.2015.07.030.
- [21] Zenk, C.H., Neumeier, S., Engl, N.M., Fries, O., Dolotko, S.G., Weiser, M., Virtanen, S. & Göken, M. (2016). Intermediate Co/Ni-base model superalloys-thermophysical properties, creep and oxidation. *Scripta Materialia*. 112, 83-86. DOI: 10.1016/j.scriptamat.2015.09.018.
- [22] Mikuszewski, T., Tomaszewska, A., Moskal, G., Migas, D. & Niemiec D. (2017). Characterization of primary microstructure of  $\gamma-\gamma'$  Co-Al-W cobalt-based superalloy. *Inżynieria Materiałowa (Materials Engineerig.)* 5, 217-223. DOI:10.15199/28.2017.5.3